

Elucidation and Pharmacological Targeting of Novel Molecular Drivers of Follicular Lymphoma Progression

Brygida Bisikirska¹, Mukesh Bansal¹, Yao Shen¹, Julie Teruya-Feldstein^{2,3}, Raju Chaganti⁴, and Andrea Califano¹

Abstract

Follicular lymphoma, the most common indolent subtype of non-Hodgkin lymphoma, is associated with a relatively long overall survival rate ranging from 6 to 10 years from the time of diagnosis. However, in 20% to 60% of follicular lymphoma patients, transformation to aggressive diffuse large B-cell lymphoma (DLBCL) reduces median survival to only 1.2 years. The specific functional and genetic determinants of follicular lymphoma transformation remain elusive, and genomic alterations underlying disease advancement have only been identified for a subset of cases. Therefore, to identify candidate drivers of follicular lymphoma transformation, we performed systematic analysis of a B-cell-specific regulatory model exhibiting follicular lymphoma transformation signatures using the Master Regulator

Inference algorithm (MARINA). This analysis revealed *FOXM1*, *TFDP1*, *ATF5*, *HMGAI*, and *NFYB* to be candidate master regulators (MR) contributing to disease progression. Accordingly, validation was achieved through synthetic lethality assays in which RNAi-mediated silencing of MRs individually or in combination reduced the viability of (14;18)-positive DLBCL (t-DLBCL) cells. Furthermore, specific combinations of small-molecule compounds targeting synergistic MR pairs induced loss of viability in t-DLBCL cells. Collectively, our findings indicate that MR analysis is a valuable method for identifying bona fide contributors to follicular lymphoma transformation and may therefore guide the selection of compounds to be used in combinatorial treatment strategies. *Cancer Res*; 76(3); 664–74. ©2015 AACR.

Introduction

Follicular lymphoma is the second most common non-Hodgkin lymphoma (NHL) subtype, right after diffuse large B-cell lymphoma (DLBCL), comprising about 22% of the annually diagnosed cases (1). Follicular lymphoma is generally diagnosed in elderly patients (>60 years of age) and is a slow-progressing neoplasm, with a median survival rate of 10 years. Despite an overall indolent course and some improvement in overall survival by rituximab-based therapy (2), follicular lymphoma remains an incurable disease. The canonical t(14;18)(q32;q21) chromosomal translocation represents the most frequent genetic alteration of this disease, detected in the vast majority of these tumors, leading to aberrant expression of the antiapoptotic protein BCL2 (3). However, this alteration alone is insufficient for tumor initiation, as the translocation is also found in healthy individuals (4). Over time, follicular lymphoma transforms to more aggressive B-cell

lymphomas, predominantly DLBCL, an event representing the hallmark of aggressive disease and poor prognosis. The frequency of histologic transformation in patients initially diagnosed with follicular lymphoma ranges from 20% to 60% depending on clinical and pathologic criteria, with median survival dropping to 1.2 years following transformation (5).

The molecular events leading to follicular lymphoma transformation are poorly characterized. Although, several genomic alterations have been associated with follicular lymphoma transformation, including *TP53* mutation, *MYC* rearrangement, *REL* amplification, and *CDKN2A/CDKN2B* deletion (6), these represent approximately 23% of all transformed follicular lymphoma cases (7). In addition to genetic alterations (8–10), epigenetic mechanisms (11) and microenvironment signals (12) have also been implicated in follicular lymphoma transformation, contributing to a relatively large, heterogeneous, and poorly understood molecular landscape.

Our recent elucidation of master regulators (MR) of glioma, prostate cancer, and germinal center reaction (13–15) suggests that distinct molecular events may induce aberrant activation of a relatively small number of MR genes, representing the causal, functional drivers of established follicular lymphoma transformation signature (16). Thus, to identify such candidate functional drivers of follicular lymphoma transformation, we interrogated an established human B-cell regulatory network, assembled from a large collection of normal and tumor-related gene expression profiles (GEP) using the ARACNe algorithm (17). This approach has been highly successful in discovering novel mechanisms of tumorigenesis and tumor progression, including synergistic gene–gene interactions that could not be elucidated by more conventional analytic approaches (13–15, 18).

¹Department of Systems Biology, Columbia University, New York, New York. ²Department of Pathology, Memorial Sloan-Kettering Cancer Center, New York, New York. ³Department of Pathology, Icahn School of Medicine at Mount Sinai, New York, New York. ⁴Cell Biology Program, Memorial Sloan-Kettering Cancer Center, New York, New York.

Note: Supplementary data for this article are available at Cancer Research Online (<http://cancerres.aacrjournals.org/>).

B. Bisikirska and M. Bansal authors contributed equally to this article.

Corresponding Author: Andrea Califano, Columbia University, 1130 St. Nicholas Ave., New York, NY 10032. Phone: 212-851-5183; Fax 212-851-4630; E-mail: ac2248@cumc.columbia.edu

doi: 10.1158/0008-5472.CAN-15-0828

©2015 American Association for Cancer Research.

The analysis identified novel candidate follicular lymphoma transformation MRs that were experimentally validated, including synthetic-lethal pairs, whose RNAi-mediated cosilencing collapsed the follicular lymphoma transformation signature and induced significant viability reduction. FDA-approved drugs computationally predicted as B-cell-specific inhibitors of these MRs were shown to induce t-DLBCL cell death, both individually and in combination.

The proposed drug prioritization methodology is highly general, relying only on the availability of a cell-specific regulatory model and disease-relevant small-molecule signatures. This paves the road to a more efficient precision medicine pipeline for the simultaneous and systematic prioritization of small-molecule compounds for either single-agent or combination therapy.

Materials and Methods

Cell lines, antibodies, and reagents

CB33, SUDHL4, and SUDHL6 cells provided by R. Dalla-Favera (Columbia University, New York, NY) were maintained in Iscove's Modified Dulbecco Medium (Life Technologies), supplemented with 10% FBS (Gemini) and antibiotics. The HF1 follicular cell line provided by R. Levy (Stanford University, Stanford, CA) was maintained in DMEM (Life Technologies), supplemented with 10% FBS and antibiotics. Cells were tested negative for mycoplasma. Cells were not further authenticated. Antibodies: rabbit anti-MYC (XP; Cell Signaling Technology); rabbit anti-FOXM1 and mouse anti-GAPDH (Santa Cruz Biotechnology); rabbit anti-HMGA1, anti-ATF5, anti-NFYB, and mouse anti-TFDP1 (Abcam). Alprostadil, clemastine, cytarabine, and troglitazone (Tocris) and econazole nitrate and promazine hydrochloride (Sigma) were reconstituted in DMSO (Sigma).

Gene silencing, qRT-PCR, and microarray assays

Gene silencing was performed using smart-pool siRNA (Dharmacon) delivered by 96-well Shuttle nucleoporation system (Amaxa) according to the manufacturer's instructions (Lonza). Detailed information on nucleoporation, qRT-PCR, and microarray assays is included in Supplementary Methods. All microarray data have been submitted to Gene Expression Omnibus (www.ncbi.nlm.nih.gov/geo; accession number GSE66714).

Cell viability

Cell viability was evaluated by PrestoBlue staining according to the manufacturer's instructions (Invitrogen). Fluorescence was measured using VICTOR 3V Plate Reader (Perkin Elmer). Small-molecule screening was performed using the CellTiter-Glo Luminescent Cell Viability Assay (Promega) in the Columbia HTS Facility. Cells were plated in 384-well plates, 24 hours prior to treatment with serial dilutions of the single compounds. Cell viability was analyzed at 48 hours to assess compound toxicity (Supplementary Fig. S4).

Tissue microarray analysis

Tissue microarray analysis (TMA) construction, diagnostic staining for GCB-origin markers, FISH analysis for t(14;18), and immunohistochemical staining for MRs were done in the Department of Pathology at Memorial Sloan-Kettering Cancer Center (New York, NY) according to ref. 19.

Computational and statistical methods

Classification of patient samples and cell lines by MYC activity. GEP patient samples were obtained from Dataset 1 (16) and Dataset 2 (20). Samples were classified as "low" and "high MYC activity" by clustering methods using MYC targets obtained from ref. 16. An outlier in the cluster analysis was excluded from further analysis. To classify cell lines for experimental validation by MYC activity, we performed clustering analysis using MYC targets on 61 samples from ref. 21. This dataset contained 38 follicular lymphoma samples, 13 transformed DLBCL samples (selected on the basis of BCL2 translocation), 10 normal GCB, 3 DLBCL cell lines (SUDHL4, SUDHL6, and VAL), and LCL-CB33.

Master Regulator Inference algorithm. We conducted MR analysis independently for "high activity MYC" and "low activity MYC" for Dataset 1 (16) and Dataset 2 (20) samples. Dataset 1 contains 6 paired samples in each group, whereas Dataset 2 has 5 and 7 paired samples in "high activity MYC" and "low activity MYC," respectively.

Computation of similarity between drug treatment and siRNA signatures. We used Gene Set Enrichment Analysis (GSEA; ref. 22) to assess drug signature similarity, based on enrichment of the 200 most upregulated genes and 200 most repressed genes from signature A in the other signature B, and *vice versa*. Enrichment scores were averaged to obtain a single metric and associated similarity *P* value.

Fisher exact test. Fisher exact test was used to assess MR overlap from each dataset (Table 1), independently for "high" and "low" MYC activity samples and to test whether specific MR proteins have positive/negative expression in DLBCL versus follicular lymphoma TMAs (Table 2).

Results

Inference of MRs of follicular lymphoma transformation

To infer candidate MRs of follicular lymphoma → DLBCL transformation (henceforth follicular lymphoma transformation), we used the Master Regulator Inference algorithm (MARINa; refs. 13–15). MARINa assessed the relevance of a transcriptional factor as a candidate MR of follicular lymphoma transformation by evaluating whether its transcriptional targets are highly enriched in genes differentially expressed in patient samples following transformation. Indeed, if aberrant activity of a transcriptional factor was responsible for transformation, then its activated and

Table 1. Overlap of MRs inferred by MARINa from different datasets

Subtype	MR mode	Dataset 1	Dataset 2	Overlap	<i>P</i>	Integrated <i>P</i>
MYC high	Activated MR	13	17	10	2.00E-07	2.00E-03
	Repressed MR	5	10	2	1.30E-01	
MYC low	Activated MR	5	6	5	2.00E-06	2.00E-03
	Repressed MR	20	25	12	1.00E-03	
All samples	Activated MR	9	12	6	3.00E-05	6.70E-02
	Repressed MR	23	17	10	2.00E-03	

Abbreviation: MR, master regulator.

Table 2. MR protein expression in follicular lymphoma and DLBCL patients' samples by TMA analysis

MR	Subtype	Samples (n)	Positive, n (%)	Negative, n (%)	P
HMGA1	DLBCL-GC	19	13 (68%)	6 (32%)	7.00E-10
	FL	58	0 (0%)	58 (100%)	
	DLBCL t(14;18)	5	5 (100%)	0 (0%)	2.20E-03
TFDP1	FL t(14;18)	6	0 (0%)	6 (100%)	
	DLBCL-GC	20	4 (20%)	16 (80%)	7.00E-01
	FL	75	17 (23%)	58 (77%)	
FOXM1	DLBCL t(14;18)	5	3 (60%)	2 (40%)	4.50E-02
	FL t(14;18)	7	0 (0%)	7 (100%)	
	DLBCL-GC	18	16 (89%)	2 (11%)	5.90E-05
NFYB	FL	88	33 (38%)	55 (62%)	
	DLBCL t(14;18)	4	3 (75%)	1 (25%)	5.30E-01
	FL t(14;18)	7	4 (57%)	3 (43%)	
ATF5	DLBCL-GC	18	7 (39%)	11 (61%)	6.20E-01
	FL	101	40 (40%)	61 (60%)	
	DLBCL t(14;18)	4	3 (75%)	1 (25%)	9.00E-02
ATF5	FL t(14;18)	7	1 (14%)	6 (85%)	
	DLBCL-GC	18	17 (94%)	1 (6%)	1.20E-07
	FL	81	22 (27%)	59 (73%)	
ATF5	DLBCL t(14;18)	4	4 (100%)	0 (0%)	3.00E-03
	FL t(14;18)	7	0 (0%)	7 (100%)	

Abbreviations: FL, follicular lymphoma; n, number; TMA, tissue microarray.

repressed targets should be overexpressed and underexpressed following transformation, respectively (Fig. 1). Prior data from glioma (13) and prostate cancer (14) studies show that top candidate MRs are highly enriched in genes eliciting essentiality or synthetic lethality. In addition, RNAi-mediated silencing of MRs should at least partially revert the follicular lymphoma transformation signature (13, 14).

As a regulatory model in this study, we used an ARACNe-inferred interactome for human B cells (21). Follicular lymphoma transformation signatures were defined using patient-matched GEPs from 12 patient biopsies at follicular lymphoma diagnosis and following transformation (Dataset 1; ref. 16). As reported, patient signatures were stratified into two distinct molecular subtypes, representing high and low MYC activity, respectively

(16). Thus, we performed independent MR analysis for each subtype (Fig. 2A and B; Supplementary Table S1A and S1B). Results were compared with equivalent MARINA analysis of an independent dataset (Dataset 2; ref. 20), comprising 12 additional patient-matched biopsies before and after transformation (Supplementary Table S1C and S1D). Despite only marginal significance (10% overlap in differentially expressed genes, $P \leq 0.05$), which is generally the case when the same phenotype is profiled by different laboratories using different technologies (13, 23), MRs inferred from these datasets were almost perfectly overlapping (77% identical MRs in the top 13, $P = 0.01$ by Fisher exact test), for both the high and the low MYC activity groups (Table 1). This is consistent with previous reports on the algorithm; see refs. 13 and 23 for details.

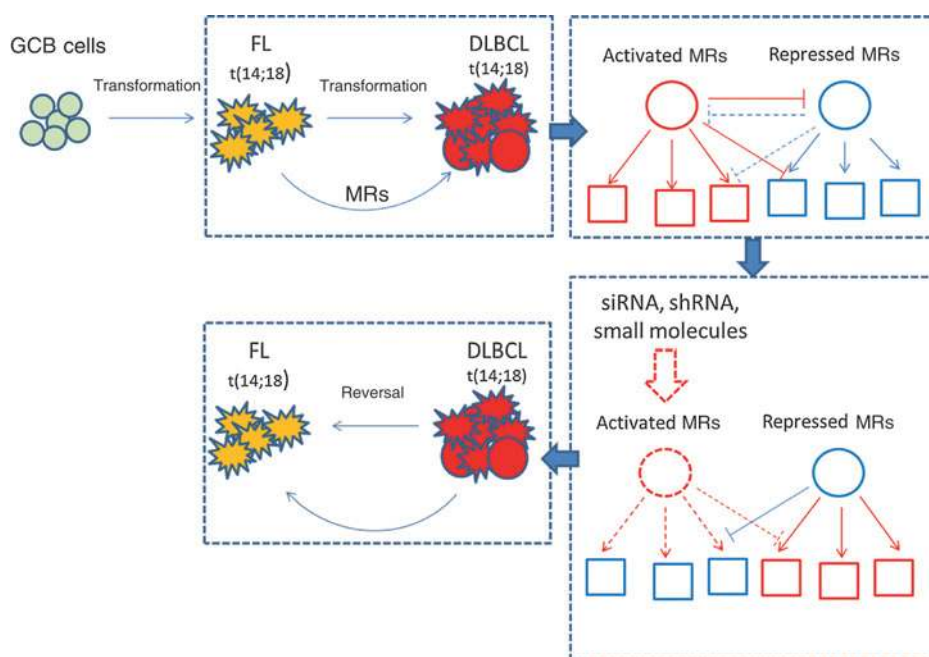


Figure 1. Model of follicular lymphoma transformation to DLBCL and experimental approach to abrogate transformed gene signature. GCB-derived aberrant follicular lymphoma cells after acquiring new oncogenic events undergo further transformation to DLBCL. These new aberrations cause erroneous downstream signaling of genes called MRs. Targeting of activated MR by siRNA/shRNA silencing or small-molecule inhibition should impair their regulatory function and abrogate the follicular lymphoma-transformed signature.

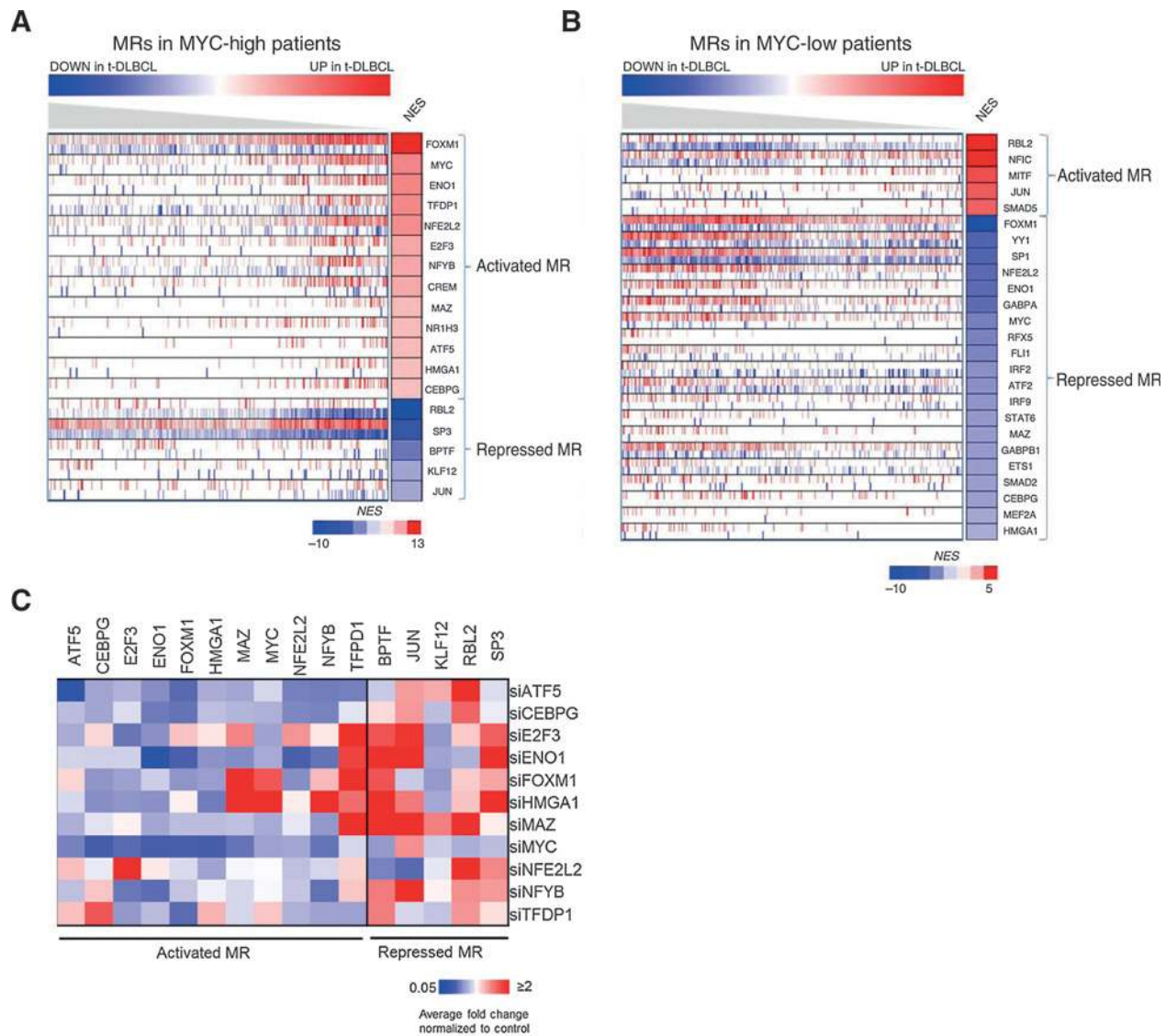


Figure 2. MR inference and mRNA expression after silencing of activated MRs in SUDHL6 cell line. A, MR of high MYC activity patients. B, MR of low MYC activity patients. Genes are sorted by NES; red, activated MR; blue, repressed MR. C, qRT-PCR analysis of MR mRNA levels at 20 hours after siRNA silencing in SUDHL6. Relative mRNA expression levels of activated MR and repressed MR were normalized to GAPDH. Heatmap represents average fold change normalized to control nontarget siRNA. Blue, downregulation; white, no change; red, upregulation (Supplementary Table S2).

Activated MRs are functional drivers of the follicular lymphoma transformation signature

MARINA identified both activated and repressed candidate MRs of follicular lymphoma transformation (Fig. 2; Supplementary Table S1A and S1B). To experimentally validate these results, we concentrated on the high MYC activity subtype, including 13 activated (*FOXM1*, *MYC*, *ENO1*, *TFPD1*, *NFE2L2*, *E2F3*, *NFYB*, *CREM*, *MAZ*, *NR1H3*, *ATF5*, *HMGA1*, *CEBPG*) and 5 repressed MRs (*SP3*, *JUN*, *BPTF*, *RBL2*, *KLF12*; Supplementary Table S1A). We selected two t(14;18)-positive DLBCL cell lines, SUDHL6 (24) and SUDHL4 (henceforth t-DLBCL cells; ref. 25), representing germinal center B-cell type (GCB) tumors, harboring the canonical BCL2 translocation t(14;18)(q32;q21), the follicular lymphoma-derived cell line HF1 (26), and as a control an

immortalized lymphoblastoid cell line LCL-CB33 (27). There are no confirmed cell lines representative of transformed follicular lymphoma. As a result, we used the t(14;18)-positive DLBCL cell lines as the model that best recapitulates the aberrant activity of the MRs we have identified from the analysis of transformed follicular lymphoma in patients. SUDHL6 and SUDHL4 cells clustered with high MYC activity follicular lymphoma-transformed patients (Supplementary Fig. S1A and S1B). mRNA expression levels of activated MRs were evaluated by qRT-PCR in all B-lymphoma cell lines (Supplementary Fig. S2A). Two genes, *NF1H3* and *CREM*, were excluded from the study due to insufficient mRNA expression and availability of Dharmacon library siRNAs, respectively. Activated MRs were systematically silenced by nucleoporation with the targeting siRNA pool in

Downloaded from <http://aacrjournals.org/cancerres/article-pdf/76/3/664/2744531/664.pdf> by guest on 24 August 2022

SUDHL6 cells (Supplementary Fig. S2B). These express high levels of MYC protein and overall highest levels of activated MR mRNA, among all tested DLBCL cell lines (Supplementary Fig. S2A). As expected, individual MR silencing, confirmed by qRT-PCR, significantly affected the expression of several other MARINA-inferred MRs, (Fig. 2C; Supplementary Table S2), suggesting cooperative activity, as a regulatory module, and supporting their inference as functional drivers of follicular lymphoma transformation.

Specifically, individual silencing of activated MR inhibited and activated expression of several other activated and repressed MRs, respectively, consistent with their inference as positive regulators of follicular lymphoma transformation signature. To select dominant activated MR genes, representing the most upstream regulators in the follicular lymphoma transformation control module, we ranked them based on their overall effect on other MARINA-inferred MRs, based on qRT-PCR data (Supplementary Table S2B). Following each MR silencing, gene expression of all other MRs was log-transformed and discretized into three states: H (fold-change, FC > 0.5), L (FC < -0.5), and M for the others. Silenced MRs were ranked by average effect on all other MRs, using their discretized state. The five highest ranking MRs (*FOXM1*, *TFDP1*, *ATF5*, *HMG1*, and *NFYB*) were selected for further study (henceforth, selected MRs).

Differential MR protein expression is confirmed in patient TMAs

To assess MR protein levels in patients, we compared TMAs from patients diagnosed with DLBCL against those with follicular lymphoma, by immunostaining with specific antibodies (Supplementary Fig. S3A). TMAs were evaluated by a board-certified pathologist and scored using a two-tier scale: negative <5% and positive \geq 5% positive cells. Staining patterns were analyzed in two complementary ways. First, we compared DLBCL samples identified by common diagnostic markers used to identify GCB-like tumors (BCL2+, CD10+, BCL6+, MUM-) to follicular lymphoma samples (Fig. 3A). The analysis revealed that *HMG1*, *FOXM1*, and *ATF5* were statistically significantly overexpressed in GCB-DLBCL versus follicular lymphoma patients, whereas *TFDP1* and *NFYB* were not significant (Table 2). Next, we compared only DLBCL patients with the canonical t(14:18) translocation, as detected by FISH, to follicular lymphoma patients (Fig. 3B) to identify those more likely to represent follicular lymphoma transformation. These results confirmed that all selected MRs, including *NFYB* and *TFDP1*, had higher protein expression in follicular lymphoma-transformed patients, although the difference for *FOXM1* was not statistically significant. These results were consistent with protein expression data from the follicular lymphoma cell line HF1 compared with high MYC t-DLBCL cell lines (Supplementary Fig. S2B), suggesting that overexpression of the selected MRs in follicular lymphoma-transformed patients is associated with the process of transformation and that *TFDP1* and *NFYB* are uniquely overexpressed following follicular lymphoma transformation.

Activated MRs are synergistic drivers of DLBCL cell proliferation

A hallmark of follicular lymphoma transformation is an increase in cellular proliferation, which usually correlates with higher MYC expression and activity (20). To evaluate an involve-

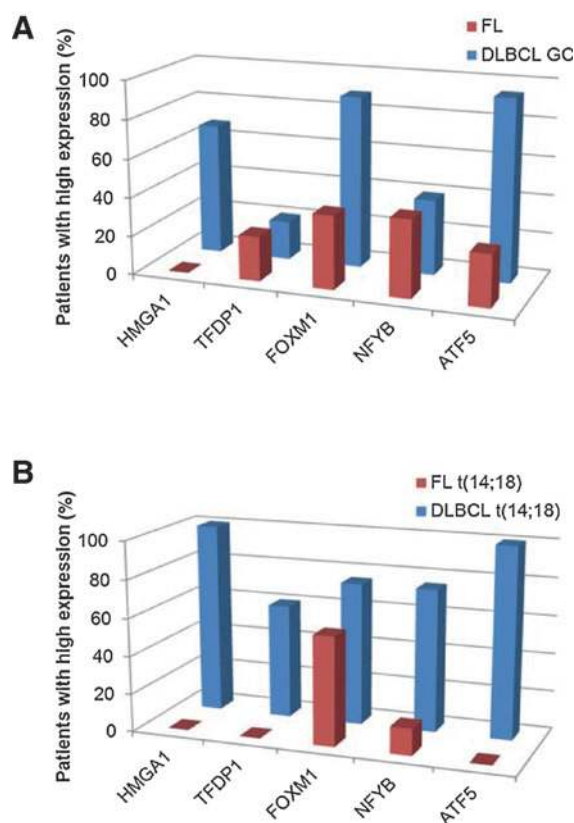


Figure 3.

Protein expression of activated MRs in DLBCL patients. Protein expression by immunohistochemical analysis in TMAs from follicular lymphoma (FL) and DLBCL patients. A, expression of MRs in follicular lymphoma and DLBCL patients defined by GCB markers. B, expression of MRs in follicular lymphoma and DLBCL patients with t(14;18) translocation. Bars represent number of patients with positive MR expression. See Table 2 for details.

ment of the selected MRs in cell proliferation *in vitro*, we assessed viability following their siRNA-pool-mediated silencing in SUDHL6, SUDHL4, HF1, and CB33 cell lines. As confirmed by Western blot analysis and qRT-PCR, significant mRNA and protein level reductions were observed at 20 hours (Supplementary Fig. S2C and S2D).

MARINA-inferred MRs frequently participate in synergistic regulation, consistent with their activity within a common regulatory module (13, 14). As a result, we also performed siRNA-mediated cosilencing of all 10 possible selected MR-pairs (Fig. 4A). siRNA targeting Ubiquitin B or AllStars Cell Death Control siRNA were used as positive controls. Results were normalized to control scrambled siRNA (NT). Confirming previous studies (13–15), while individual MR silencing (except for *ATF5*) did not significantly reduce cell viability at 24 hours, in either DLBCL cell line, MR cosilencing profoundly affected cell viability for most MR pairs, (7/10) in SUDHL6 and (10/10) in SUDHL4, supporting their role as candidate synergistic dependencies of t-DLBCL cells. In contrast, there was only minimal effect in control cells, (2/10) in HF1 cells and 0/10 in CB33 cells. This suggests that follicular lymphoma transformation results from and is dependent on the cooperative effect of multiple dysregulated transcriptional factors and not from aberrant activity of any individual one in isolation.

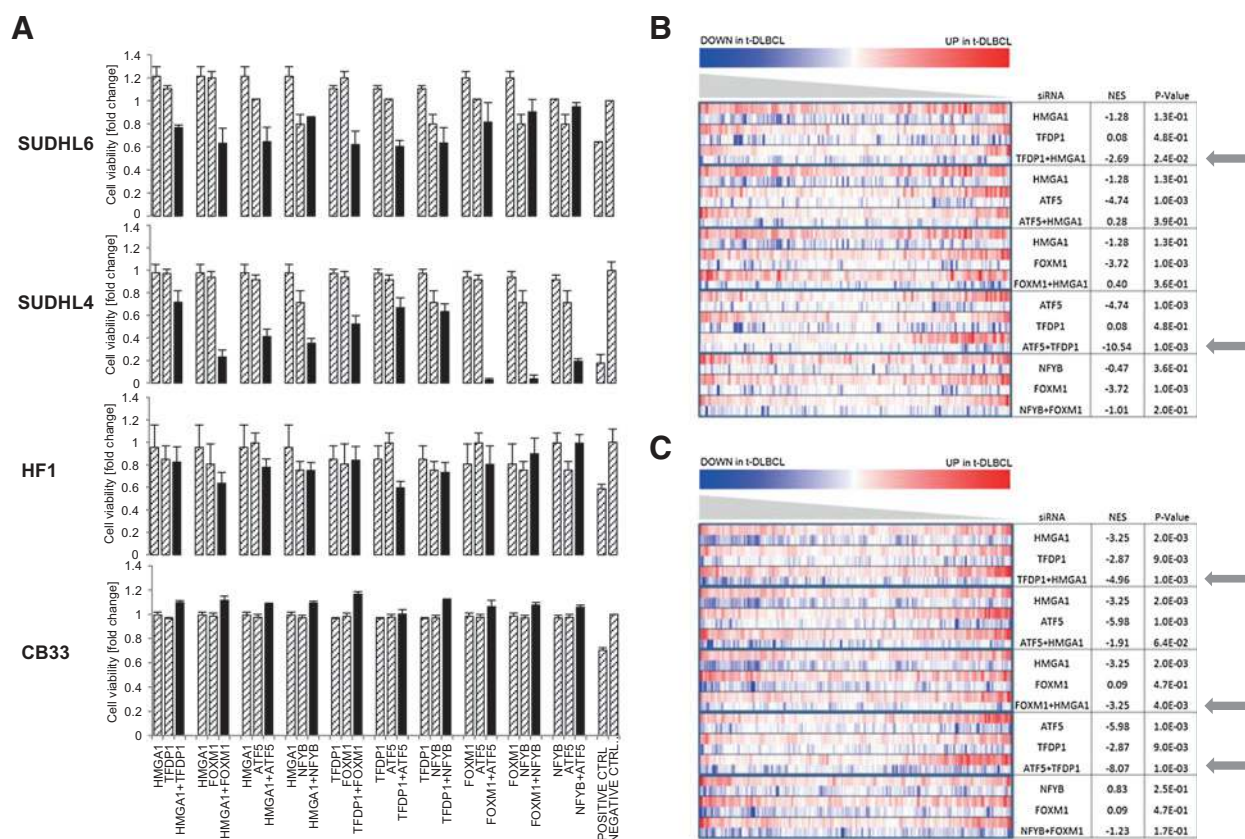


Figure 4. Synergistic MRs drive t-DLBCL cell proliferation and define transformed follicular lymphoma gene signature. A, cell viability measured by PrestoBlue at 24 hours after single and paired MRs silencing of SUDHL6, SUDHL4, HF1, and CB33 cell lines. B and C, GSEA of differentially expressed genes after MR silencing in SUDHL6 cell line in patient-derived signatures of follicular lymphoma transformation using datasets from ref. 16 and ref. 20, respectively.

Gene expression analysis of t-DLBCL cells following MR silencing

To further validate the role of inferred MRs in follicular lymphoma transformation, we analyzed the gene expression signature of t-DLBCL cells following both individual MR and MR-pair silencing. Specifically, if some of the MARINA-inferred MRs are bona fide causal determinants of follicular lymphoma transformation, their silencing should at least partially abrogate the follicular lymphoma transformation signature, with a more profound effect when MR pairs are cosilenced. To test our hypothesis, we selected the five MR pairs producing the most significant synergistic cell viability reduction in both t-DLBCL cell lines, including *HMGA1/TFDP1*, *HMGA1/ATF5*, *HMGA1/FOXM1*, *ATF5/TFDP1*, and *NFYB/FOXM1*, and performed GEPs of SUDHL6 cells at 20 hours following silencing of each MR and MR pair (Fig. 4B and C) (Supplementary Methods). Differential gene expression analysis, with respect to NT control SUDHL6 cells, was performed using a SAM test (28). We used GSEA analysis to assess whether genes differentially expressed following MR silencing were negatively enriched in genes differentially expressed in patients following follicular lymphoma transformation in the high-MYC subtype, using both independent studies (Fig. 4B and C; refs. 16, 20). We also compared normalized enrichment score (NES) for individual MR silencing versus MR-pair silencing, to further evaluate the synergistic

nature of MR regulation. Analysis of patient signatures from both datasets (16, 20) consistently identified 2 pairs (*HMGA1/TFDP1* and *ATF5/TFDP1*) as effecting the most striking reversal of t-DLBCL cell gene expression to a follicular lymphoma-like state. For both pairs, cosilencing significantly outperformed individual MR silencing, both by NES and/or P value assessment. In addition, the *HMGA1/FOXM1* pair was identified and experimentally validated as a candidate synergistic based on signatures from Dataset 2 (20). Taken together, these assays show that most MARINA-inferred MRs indeed regulate genes in the follicular lymphoma transformation signature, even though, individually, their effect is not sufficient to induce follicular lymphoma transformation signature collapse. Indeed, genes differentially expressed following individual MR silencing, including *HMGA1*, *TFDP1*, and *ATF5*, were significantly enriched in genes expressed in follicular lymphoma patients before transformation. In sharp contrast, consistent with previous results in other tumors, MR-pair silencing leads to follicular lymphoma transformation signature collapse and significant loss of cell viability at 24 hours.

Targeting follicular lymphoma transformation MRs with small-molecule perturbations

Identification of MR proteins representing novel functional drivers of tumor-related phenotypes may open relevant

Downloaded from <http://aacrjournals.org/cancerres/article-pdf/76/3/664/2744531/664.pdf> by guest on 24 August 2022

therapeutic opportunities (18). As proof of concept, we thus proceeded to assess whether B-cell-specific inhibitors of validated MRs could be systematically identified from small-molecule perturbation assays. Following the Connectivity Map rationale (29), we reasoned that the differential expression signature following MR silencing in human B cells represent an ideal multiplexed gene reporter assays to assess the activity of candidate small-molecule inhibitors of the same MR. As transcriptional factor targets are highly conserved across 18 distinct subtypes of human B cells, including follicular lymphoma and DLBCL (the rationale for using the B-cell interactome for this analysis; ref. 30), we proceeded to assess 92 compounds for which GEPs were available following perturbation of an ABC (OCI-LY3) and a GCG (OCI-LY7) DLBCL cell lines (31). Specifically, we assessed enrichment of compound-induced signatures in genes differentially expressed following siRNA-mediated silencing of validated follicular lymphoma transformation MRs in SUDHL6 cells, using a two-tail GSEA (23) to account for both over-expressed and underexpressed genes, to identify compounds

that significantly recapitulate relevant MR silencing (Supplementary Table S3A).

As individual MR silencing had little effect on tumor viability, we prioritized four compound combinations predicted to target the synergistic MR pairs inducing greatest viability reduction in SUDHL6 and SUDHL4 cells. These were tested in SUDHL4 and SUDHL6 (t-DLBCL), HF1 (follicular lymphoma), and LCL-CB33 (normal control) cells (Supplementary Table S3B). For each combination, we used a 10×10 dilution matrix, with individual compound concentrations ranging from 0.003 $\mu\text{mol/L}$ to 20 $\mu\text{mol/L}$ (Supplementary Fig. S4). Cell viability was assessed by ATP levels at 48 hours following compound treatment (see Materials and Methods). To evaluate compound synergy, we used the Excess-over-Bliss (EOB) score (Supplementary Methods), defined as a difference between the observed and predicted additive drug combination effect (Fig. 5; Supplementary Table S5). Compound pairs were considered strongly synergistic at $\text{EOB} \geq 20$. As expected, compound pairs predicted to target synergistic MRs were strongly synergistic in t-DLBCL cells but not in follicular

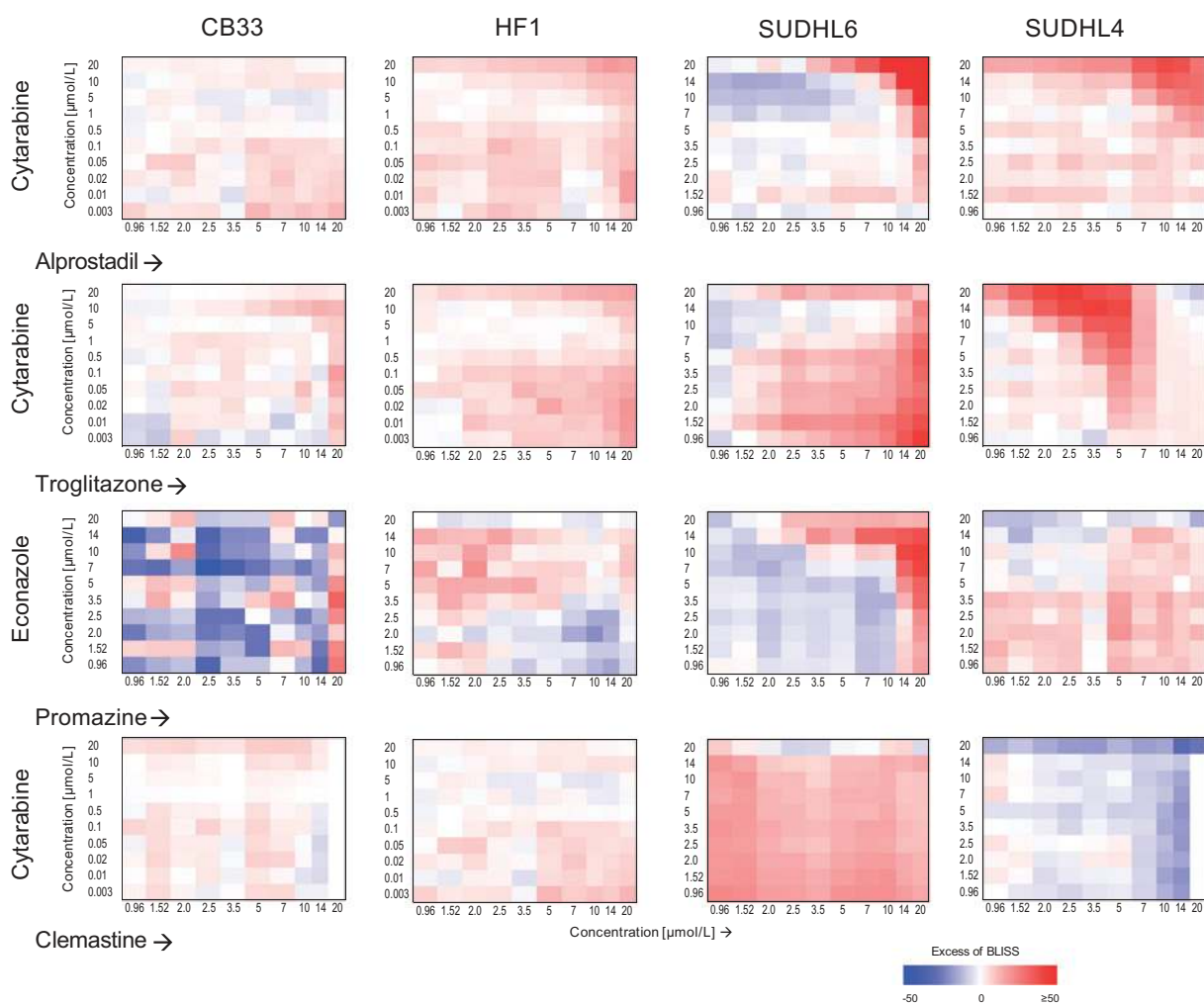


Figure 5.

Effect of drug combinations on cell viability in B-lymphoma cell lines. Cell viability of SUDHL6, SUDHL4, HF1, and CB33 cells treated with the combination of compounds for 48 hours was evaluated by ATP assay. Compound synergy is represented by EOB score; we defined $\text{EOB} \geq 20$ as strongly synergistic and $\text{EOB} \leq -20$ as strongly antagonistic. Color-coded matrices represent EOS scores; red, positive; blue, negative.

lymphoma and control cells. Among these, alprostadil/cytarabine (targeting the HMGA1/FOXM1 pair) were strongly synergistic in both t-DLBCL cell lines. Troglitazone/cytarabine (targeting the FOXM1/NFYB pair) and econazole/promazine (targeting the HMGA1/TFDP1 pair) presented stronger synergistic activity in SUDHL4 versus SUDHL6 cells and vice versa, respectively, consistent with greater viability reduction following cosilencing of the associated MR pairs. Finally, clemastine/cytarabine (both targeting FOXM1), showed no synergistic activity in any of the four cell lines, as expected.

Although the clinical relevance of these results is limited by the relatively small number of profiled compounds and by lack of *in vivo* validation, all of the four predicted compound combinations induced synergistic t-DLBCL cell death. Thus, these results represent an important proof of concept that MR analysis, combined with straightforward perturbational assays, can help identify compound combinations that are effective in abrogating tumor cell viability *in vitro*.

Discussion

Precision cancer medicine has been almost universally predicated on the use of targeted inhibitors for oncogenes harboring activating mutations, based on the "oncogene addiction" paradigm (32). Although this has been transformational for some tumors, from chronic myelogenous leukemia to lung cancer, it also presents significant limitations. Indeed, oncogene mutations are neither individually sufficient nor necessary for implementing and maintaining molecularly distinct tumor subtypes. Consistently, there are no fully penetrant genomic alterations responsible for inducing follicular lymphoma transformation of every high or low MYC subtype patient, even though the gene expression signatures of patients undergoing follicular lymphoma transformation to either subtype are virtually identical, suggesting a common, conserved functional regulators set.

As a result, we decided to approach follicular lymphoma transformation from a different and highly complementary perspective. Rather than looking for recurrent genetic or epigenetic alterations in a transformed patient cohort, we interrogated a B-cell-specific regulatory network to identify transcriptional factors that are responsible for the specific regulation of genes that are differentially expressed following patient follicular lymphoma transformation to either the low MYC or high MYC subtype. As previously shown for glioma, breast cancer, and even Alzheimer disease, and as confirmed by DIGGIT analysis (18), the MRs of follicular lymphoma transformation were downstream of most previously reported genetic alterations, including *CARD11*, *CD79A*, *CD79B*, *STAT3*, *CREBBP*, *TNFRSF14*, *SOCS1*, *BCL10*, *PRKCB*, and *PLCG2* (data not shown) (10). As a result, they represent nononcogene dependencies, as proposed in ref. 33, whose aberrant regulatory activity is the result of one or more genetic or epigenetic alterations in their upstream pathways.

Even though the MARINA algorithm has already been effectively used to elucidate novel functional drivers in glioblastoma, prostate cancer, leukemia, and breast cancer, our study presents significant novelty in two distinct areas. First, we report a novel tumor checkpoint, comprising 18 MR proteins, whose synergistic activity regulates the genes that are differentially expressed in follicular lymphoma patients following transformation. Coinhibition of activated MR pairs induces rapid and specific cell death

in t-DLBCL cells, but not in follicular lymphoma related and normal related B cells. Second, we used the MR-silencing signature to elucidate compounds that, in combinations, may induce t-DLBCL-specific cell death, opening a new avenue in precision cancer medicine, especially for phenotypes lacking a canonical targetable oncogene dependency.

Critically, both the B-cell-specific regulatory model and the follicular lymphoma transformation signatures were derived from primary patient tissue. Thus, our predictions are independent of potentially idiosyncratic cell line or mouse model dependencies and should have high likelihood of being further recapitulated *in vivo*. Our model for the transformation process is consistent with the recently proposed linear evolution model (9), suggesting that transformed follicular lymphoma originates from the dominant follicular lymphoma clone as a result of new oncogenic events. However, as MARINA analysis is agnostic to the underlying tumor progression mechanism and only predicts the regulatory proteins that become aberrantly activated as a result of these secondary events our findings would equally support alternative hypotheses, such as divergent evolution.

Confirming results from previous studies (13, 14, 18), MARINA-inferred MRs were found to be highly enriched in synthetic lethal pairs. Although several of these genes were previously reported as overexpressed in hematologic malignancies, such as *MYC* (34), *FOXM1* (35), *TFDP1* (36), and *ATF5* (37), the majority of inferred MRs were not previously causally associated with follicular lymphoma transformation nor were they shown to represent individual/synergistic dependencies of transformed DLBCL. Five of these MRs emerged as the strongest causal determinant of follicular lymphoma transformation signature, including *FOXM1*, *TFDP1*, *ATF5*, *HMGA1*, *MYC*, and *NFYB*. Interestingly, with the exception of *MYC*, these genes had been previously reported among 26 MRs of the germinal center reaction (15), suggesting that dysregulation of proteins presiding over B-cell maturation programs by a complex landscape of genetic and epigenetic alterations may be responsible for transformation of GCB-originated follicular lymphoma to DLBCL. Immunohistochemical assays in patient-derived TMAs confirmed overexpression of the five MR proteins in DLBCL patients harboring the canonical t(14;18)(q32;q21) translocation, compared with follicular lymphoma tumors.

We showed that MRs act synergistically to preserve the transformed follicular lymphoma state. Indeed, siRNA-mediated cosilencing of MR pairs, including *HMGA1/TFDP1* and *ATF5/TFDP1*, and *FOXM1/HMGA1*, had a profound effect on t-DLBCL cell viability but not on that of follicular lymphoma and lymphoblastoid cell lines. Consistently, analysis of GEPs from SUDHL6 cells following cosilencing of these MR pairs showed a significant shift toward a follicular lymphoma-like signature. Slight differences in the analyses were likely associated with the differences in Lymphochip cDNA gene sets used in these analyses (10,731 and 4,908 genes, respectively).

HMGA1/TFDP1 and *ATF5/TFDP1* pairs were consistently identified from both patient signatures. HMGA1 proteins are members of a nonhistone, chromatin-binding protein family, detected at high level during the process of embryogenesis in contrast to normal adult tissues and associated with a variety of aggressive human malignancies (reviewed in ref. 38). A recent study of HMGA1's role in reprogramming somatic cell into pluripotent stem cell (39) suggests that HMGA1 could be an important MR of neoplastic transformations, responsible for

tumor state plasticity and reprogramming. Yet, our study represents the first evidence where HMGA1 is identified as a mechanistic regulator of follicular lymphoma transformation and as a potentially synergistic cofactor. TFDP1 is an established heterodimerization partner of E2F family proteins, regulating transcriptional activity of cell-cycle progression genes (40). Both TFDP1 and E2F1 can interact and inhibit transcriptional activity of p53 and are expressed in NHLs (36). A member of the E2F family, E2F3, was also inferred as an activated MR by MARINA analysis, suggesting that these proteins may represent interacting partners in follicular lymphoma progression. Finally, ATF5 is a member of the ATF/CREB family of transcriptional factors, widely expressed in neoplastic and normal tissues; however, only in neoplastic cells was silencing of ATF5 shown to induce cell death (41). ATF5 was also associated with sensitivity to bortezomib-induced apoptosis in SUDHL6, but not SUDHL4 DLBCL cell lines (37), nonetheless it was never reported in the context of follicular lymphoma transformation.

Precise characterization of MR genes representing individual/synergistic oncogene and nononcogene dependencies of transformed DLBCL opens a range of novel opportunities for targeted pharmacologic treatment. Here we demonstrate that relevant MR inhibitors, likely operating indirectly, could be effectively inferred from the analysis of GEPs following small-molecule perturbation in representative cell lines.

Specifically, based on our previously ascertained conservation of regulatory interactions across 18 distinct human B-cell subtypes, including follicular lymphoma and DLBCL, we used GEPs of DLBCL cell lines following treatment with a library of 92 FDA-approved compounds to infer novel candidate inhibitors of follicular lymphoma transformation MRs. Our analysis identified several compound combinations that were experimentally validated, showing synergistic activity in t-DLBCL cells but not in normal or follicular lymphoma-derived cells. Remarkably, even though this study represents only a proof of concept, it prioritized cytarabine, a drug frequently used in combination therapy for the treatment of acute leukemias and lymphomas (42, 43). Indeed, high-dose cytarabine, in combination with cisplatin and dexamethasone (DHAP), etoposide, cisplatin, and methylprednisolone (ESHAP), is representative of key chemotherapeutic regimens for NHL and Hodgkin lymphoma treatment (43). Our study identified the novel synergistic interaction of cytarabine and alprostadil (Prostaglandin E1) or troglitazone to induce cell death in DLBCL cells but not in follicular lymphoma and control cells. Prostaglandins are hormone-like lipid metabolites, playing a key role in inflammatory response (44). Although prostaglandins are associated with wide range of cancers they were also shown to induce apoptosis in human leukemia cell lines (45). Troglitazone is an anti-inflammatory drug, initially used for treatment of patients with type 2 diabetes. It activates PPARs and decreases NF- κ B (46). As PPAR γ agonists were shown to induce apoptosis in human B lymphomas (47), troglitazone could prove a very realistic choice in transformed follicular lymphoma. Because of adverse events, this drug was withdrawn from the market in 2000. Yet, new troglitazone derivatives with lower toxicity and anti-

proliferative activity are now emerging (48). Two other compounds, econazole nitrate and promazine hydrochloride, showed synergy in the SUDHL6 cell line. Econazole is best known as an antifungal medication but there is increasing evidence that it may also have anticancer properties (49). Moreover, it was shown that sensitivity to econazole is specifically mediated by MYC in the HL60 cell line. Indeed, MYC-negative cells were resistant to this agent (50).

Taken together, these data suggest that the systematic, network-based identification of MR genes may represent an alternative and highly complementary approach to the targeting of classic oncogene dependencies. Once these dependencies are identified, their small-molecule inhibitors, including both individual drugs and synergistic drug combinations, can be effectively prioritized. If further validated, such an approach would significantly extend the reach of precision cancer medicine, especially as the analyses performed in this article can be performed in hours to days using high-performance computing platforms. This would allow the efficient prioritization of compound and compound combinations to treat individual tumors.

Disclosure of Potential Conflicts of Interest

R. Chaganti is a director, consultant; has ownership interest (including patents) and is a consultant/advisory board member for Cancer Genetics, Inc. A. Califano is a founder and SAB chair at Darwin Health; reports receiving a commercial research grant from Merrimack; has ownership interest (including patents) in Darwin Health; and is a consultant/advisory board member for Cancer Genetics, Inc. and Dow Agro. No potential conflicts of interest were disclosed by the other authors.

Authors' Contributions

Conception and design: B. Bisikirska, M. Bansal, A. Califano

Development of methodology: M. Bansal, A. Califano

Acquisition of data (provided animals, acquired and managed patients, provided facilities, etc.): B. Bisikirska, M. Bansal, J. Teruya-Feldstein, R. Chaganti

Analysis and interpretation of data (e.g., statistical analysis, biostatistics, computational analysis): B. Bisikirska, M. Bansal, Y. Shen

Writing, review, and/or revision of the manuscript: B. Bisikirska, M. Bansal, Y. Shen, A. Califano

Study supervision: A. Califano

Acknowledgments

The authors thank Riccardo Dalla-Favera and Laura Pasqualucci for providing cell lines (CB33, SUDHL4, and SUDHL6) and gene expression data for 226 B-cell samples including cell lines and FISH data for BCL2 translocation in DLBCL samples.

Grant Support

This work was supported by the CTD2 (Cancer Target Discovery and Development; 5U01CA168426) and the MAGNet (Multiscale Analysis of Genomic and Cellular Networks - <http://magnet.c2b2.columbia.edu/5U54CA121852>) grants.

The costs of publication of this article were defrayed in part by the payment of page charges. This article must therefore be hereby marked *advertisement* in accordance with 18 U.S.C. Section 1734 solely to indicate this fact.

Received March 30, 2015; revised October 8, 2015; accepted October 21, 2015; published OnlineFirst November 20, 2015.

References

1. A clinical evaluation of the International Lymphoma Study Group classification of non-Hodgkin's lymphoma. The Non-Hodgkin's Lymphoma Classification Project. *Blood* 1997;89:3909-18.
2. Guirguis HR, Cheung MC, Piliotis E, Spaner D, Berinstein NL, Imrie K, et al. Survival of patients with transformed lymphoma in the rituximab era. *Ann Hematol* 2014;93:1007-14.

3. Vaandrager JW, Schuurin E, Raap T, Philippo K, Kleiverda K, Kluin P. Interphase FISH detection of BCL2 rearrangement in follicular lymphoma using breakpoint-flanking probes. *Genes Chromosomes Cancer* 2000;27:85–94.
4. Limpens J, Stad R, Vos C, de Vlaam C, de Jong D, van Ommen GJ, et al. Lymphoma-associated translocation t(14;18) in blood B cells of normal individuals. *Blood* 1995;85:2528–36.
5. Montoto S, Davies AJ, Matthews J, Calaminici M, Norton AJ, Amess J, et al. Risk and clinical implications of transformation of follicular lymphoma to diffuse large B-cell lymphoma. *J Clin Oncol* 2007;25:2426–33.
6. Freedman AS. Biology and management of histologic transformation of indolent lymphoma. *Hematology Am Soc Hematol Educ Program* 2005:314–20.
7. Goff LK, Neat MJ, Crawley CR, Jones L, Jones E, Lister TA, et al. The use of real-time quantitative polymerase chain reaction and comparative genomic hybridization to identify amplification of the REL gene in follicular lymphoma. *Br J Haematol* 2000;111:618–25.
8. Berglund M, Enblad G, Thunberg U, Amini RM, Sundstrom C, Roos G, et al. Genomic imbalances during transformation from follicular lymphoma to diffuse large B-cell lymphoma. *Mod Pathol* 2007;20:63–75.
9. Pasqualucci L, Khiabanian H, Fangazio M, Vasishtha M, Messina M, Holmes AB, et al. Genetics of follicular lymphoma transformation. *Cell Rep* 2014;6:130–40.
10. Okosun J, Bodor C, Wang J, Araf S, Yang CY, Pan C, et al. Integrated genomic analysis identifies recurrent mutations and evolution patterns driving the initiation and progression of follicular lymphoma. *Nat Genet* 2014;46:176–81.
11. Hayslip J, Montero A. Tumor suppressor gene methylation in follicular lymphoma: a comprehensive review. *Mol Cancer* 2006;5:44.
12. Rawal S, Chu F, Zhang M, Park HJ, Nattamai D, Kannan S, et al. Cross talk between follicular Th cells and tumor cells in human follicular lymphoma promotes immune evasion in the tumor microenvironment. *J Immunol* 2013;190:6681–93.
13. Carro MS, Lim WK, Alvarez MJ, Bollo RJ, Zhao X, Snyder EY, et al. The transcriptional network for mesenchymal transformation of brain tumours. *Nature* 2010;463:318–25.
14. Aytes A, Mitrofanova A, Lefebvre C, Alvarez MJ, Castillo-Martin M, Zheng T, et al. Cross-species regulatory network analysis identifies a synergistic interaction between FOXM1 and CENPF that drives prostate cancer malignancy. *Cancer Cell* 2014;25:638–51.
15. Lefebvre C, Rajbhandari P, Alvarez MJ, Bandaru P, Lim WK, Sato M, et al. A human B-cell interactome identifies MYB and FOXM1 as master regulators of proliferation in germinal centers. *Mol Syst Biol* 2010;6:377.
16. Lossos IS, Alizadeh AA, Diehn M, Warnke R, Thorstenson Y, Oefner PJ, et al. Transformation of follicular lymphoma to diffuse large-cell lymphoma: alternative patterns with increased or decreased expression of c-myc and its regulated genes. *Proc Natl Acad Sci U S A* 2002;99:8886–91.
17. Basso K, Margolin AA, Stolovitzky G, Klein U, Dalla-Favera R, Califano A. Reverse engineering of regulatory networks in human B cells. *Nat Genet* 2005;37:382–90.
18. Chen JC, Alvarez MJ, Talos F, Dhruv H, Rieckhof GE, Iyer A, et al. Identification of causal genetic drivers of human disease through systems-level analysis of regulatory networks. *Cell* 2014;159:402–14.
19. Hedvat CV, Hegde A, Chaganti RS, Chen B, Qin J, Filippa DA, et al. Application of tissue microarray technology to the study of non-Hodgkin's and Hodgkin's lymphoma. *Hum Pathol* 2002;33:968–74.
20. Davies AJ, Rosenwald A, Wright G, Lee A, Last KW, Weisenburger DD, et al. Transformation of follicular lymphoma to diffuse large B-cell lymphoma proceeds by distinct oncogenic mechanisms. *Br J Haematol* 2007;136:286–93.
21. Basso K, Saito M, Sumazin P, Margolin AA, Wang K, Lim WK, et al. Integrated biochemical and computational approach identifies BCL6 direct target genes controlling multiple pathways in normal germinal center B cells. *Blood* 2010;115:975–84.
22. Subramanian A, Tamayo P, Mootha VK, Mukherjee S, Ebert BL, Gillette MA, et al. Gene set enrichment analysis: a knowledge-based approach for interpreting genome-wide expression profiles. *Proc Natl Acad Sci U S A* 2005;102:15545–50.
23. Lim WK, Lyashenko E, Califano A. Master regulators used as breast cancer metastasis classifiers. *Pac Symp Biocomput* 2009;14:504–15.
24. Siminovitch KA, Jensen JP, Epstein AL, Korsmeyer SJ. Immunoglobulin gene rearrangements and expression in diffuse histiocytic lymphomas reveal cellular lineage, molecular defects, and sites of chromosomal translocation. *Blood* 1986;67:391–7.
25. Bakhshi A, Jensen JP, Goldman P, Wright JJ, McBride OW, Epstein AL, et al. Cloning the chromosomal breakpoint of t(14;18) human lymphomas: clustering around JH on chromosome 14 and near a transcriptional unit on 18. *Cell* 1985;41:899–906.
26. Knuutila S, Klefstrom J, Szymanska J, Lakkala T, Peltomaki P, Eray M, et al. Two novel human B-cell lymphoma lines of lymphatic follicle origin: cytogenetic, molecular genetic and histopathological characterisation. *Eur J Haematol* 1994;52:65–72.
27. Lombardi L, Newcomb EW, Dalla-Favera R. Pathogenesis of Burkitt lymphoma: expression of an activated c-myc oncogene causes the tumorigenic conversion of EBV-infected human B lymphoblasts. *Cell* 1987;49:161–70.
28. Tusher VG, Tibshirani R, Chu G. Significance analysis of microarrays applied to the ionizing radiation response. *Proc Natl Acad Sci U S A* 2001;98:5116–21.
29. Lamb J, Crawford ED, Peck D, Modell JW, Blat IC, Wrobel MJ, et al. The Connectivity Map: using gene-expression signatures to connect small molecules, genes, and disease. *Science* 2006;313:1929–35.
30. Mani KM, Lefebvre C, Wang K, Lim WK, Basso K, Dalla-Favera R, et al. A systems biology approach to prediction of oncogenes and molecular perturbation targets in B-cell lymphomas. *Mol Syst Biol* 2008;4:169.
31. Woo HJ, Shimoni Y, Yang SW, Subramanian P, Iyer A, Nicoletti P. Elucidating compound mechanism of action by network dysregulation analysis in perturbed cells. *Cell* 2015;162:441–51.
32. Weinstein IB. Cancer. Addiction to oncogenes—the Achilles heel of cancer. *Science* 2002;297:63–4.
33. Luo J, Solimini NL, Elledge SJ. Principles of cancer therapy: oncogene and non-oncogene addiction. *Cell* 2009;136:823–37.
34. Yano T, Jaffe ES, Longo DL, Raffeld M. MYC rearrangements in histologically progressed follicular lymphomas. *Blood* 1992;80:758–67.
35. Uddin S, Hussain AR, Ahmed M, Siddiqui K, Al-Dayel F, Bavi P, et al. Overexpression of FoxM1 offers a promising therapeutic target in diffuse large B-cell lymphoma. *Haematologica* 2012;97:1092–100.
36. Chan JA, Olvera M, Lai R, Naing W, Rezk SA, Brynes RK. Immunohistochemical expression of the transcription factor DP-1 and its heterodimeric partner E2F-1 in non-Hodgkin lymphoma. *Appl Immunohistochem Mol Morphol* 2002;10:322–6.
37. Shringarpure R, Catley L, Bhole D, Burger R, Podar K, Tai YT, et al. Gene expression analysis of B-lymphoma cells resistant and sensitive to bortezomib. *Br J Haematol* 2006;134:145–56.
38. Shah SN, Resar LM. High mobility group A1 and cancer: potential biomarker and therapeutic target. *Histol Histopathol* 2012;27:567–79.
39. Shah SN, Kerr C, Cope L, Zambidis E, Liu C, Hillion J, et al. HMGA1 reprograms somatic cells into pluripotent stem cells by inducing stem cell transcriptional networks. *PLoS One* 2012;7:e48533.
40. O'Connor DJ, Lam EW, Griffin S, Zhong S, Leighton LC, Burbidge SA, et al. Physical and functional interactions between p53 and cell cycle co-operating transcription factors, E2F1 and DP1. *EMBO J* 1995;14:6184–92.
41. Monaco SE, Angelastro JM, Szabolcs M, Greene LA. The transcription factor ATF5 is widely expressed in carcinomas, and interference with its function selectively kills neoplastic, but not nontransformed, breast cell lines. *Int J Cancer* 2007;120:1883–90.
42. Bishop JF, Matthews JP, Young GA, Bradstock K, Lowenthal RM. Intensified induction chemotherapy with high dose cytarabine and etoposide for acute myeloid leukemia: a review and updated results of the Australian Leukemia Study Group. *Leuk Lymphoma* 1998;28:315–27.
43. McCarthy J, Gopal AK. Successful use of full-dose dexamethasone, high-dose cytarabine, and cisplatin as part of initial therapy in non-hodgkin and hodgkin lymphoma with severe hepatic dysfunction. *Clin Lymphoma Myeloma* 2009;9:167–70.
44. Riccotti E, FitzGerald GA. Prostaglandins and inflammation. *Arterioscler Thromb Vasc Biol* 2011;31:986–1000.
45. Soleymani Fard S, Jeddi Tehrani M, Ardekani AM. Prostaglandin E2 induces growth inhibition, apoptosis and differentiation in T and B cell-derived acute lymphoblastic leukemia cell lines (CCRF-CEM and Nalm-6). *Prostaglandins Leukot Essent Fatty Acids* 2012;87:17–24.
46. Wolffenbuttel BH, Graal MB. New treatments for patients with type 2 diabetes mellitus. *Postgrad Med J* 1996;72:657–62.

47. Padilla J, Leung E, Phipps RP. Human B lymphocytes and B lymphomas express PPAR-gamma and are killed by PPAR-gamma agonists. *Clin Immunol* 2002;103:22–33.
48. Bordessa A, Colin-Cassin C, Grillier-Vuissoz I, Kuntz S, Mazerbourg S, Husson G, et al. Optimization of troglitazone derivatives as potent anti-proliferative agents: towards more active and less toxic compounds. *Eur J Med Chem* 2014;83:129–40.
49. Ho YS, Wu CH, Chou HM, Wang YJ, Tseng H, Chen CH, et al. Molecular mechanisms of econazole-induced toxicity on human colon cancer cells: G0/G1 cell cycle arrest and caspase 8-independent apoptotic signaling pathways. *Food Chem Toxicol* 2005;43:1483–95.
50. Chen X, Xu H, Yuan P, Fang F, Huss M, Vega VB, et al. Integration of external signaling pathways with the core transcriptional network in embryonic stem cells. *Cell* 2008;133:1106–17.